Neuron, Vol. 39, 513–528, July 31, 2003, Copyright ©2003 by Cell Press

Narp and NP1 Form Heterocomplexes that Function in Developmental and Activity-Dependent Synaptic Plasticity

Desheng Xu,[1,4] Carsten Hopf,[1,4,5] Radhika Reddy,[1] Richard W. Cho,[1] Liping Guo,[1] Anthony Lanahan,[1] Ronald S. Petralia,[3] Robert J. Wenthold,[3] Richard J. O'Brien,[2] and Paul Worley[1,2,*]

[1]Department of Neuroscience
[2]Department of Neurology
Johns Hopkins University School of Medicine
Baltimore, Maryland 21205
[3]Laboratory of Neurochemistry
National Institute on Deafness and Other Communication Disorders
National Institutes of Health
Bethesda, Maryland 20892

Summary

Narp is a neuronal immediate early gene that plays a role in excitatory synaptogenesis. Here, we report that native Narp in brain is part of a pentraxin complex that includes NP1. These proteins are covalently linked by disulfide bonds into highly organized complexes, and their relative ratio in the complex is dynamically dependent upon the neuron's activity history and developmental stage. Complex formation is dependent on their distinct N-terminal coiled-coil domains, while their closely homologous C-terminal pentraxin domains mediate association with AMPA-type glutamate receptors. Narp is substantially more effective in assays of cell surface cluster formation, coclustering of AMPA receptors, and excitatory synaptogenesis, yet their combined expression results in supraadditive effects. These studies support a model in which Narp can regulate the latent synaptogenic activity of NP1 by forming mixed pentraxin assemblies. This mechanism appears to contribute to both activity-independent and activity-dependent excitatory synaptogenesis.

Introduction

The discovery of agrin and the elucidation of its synaptogenic properties at the neuromuscular junction (McMahan, 1990; Sanes and Lichtman, 2001) presaged the identification of analogous factors in the CNS, including agrin (Bose et al., 2000; Ferreira, 1999; but see also Serpinskaya et al., 1999), cadherins (Bruses, 2000; Yagi and Takeichi, 2000), β-neurexin-neuroligin (Missler and Sudhof, 1998; Rao et al., 2000; Scheiffele et al., 2000), EphrinB-EphB receptor tyrosine kinase (Dalva et al., 2000), syndecan-2 (Ethell et al., 2001; Ethell and Yamaguchi, 1999), CPG15 (Cantallops et al., 2000; Nedivi et al., 1998), SynCAM (Biederer et al., 2002), and Narp (O'Brien et al., 1999; Tsui et al., 1996). These protein systems are hypothesized to contribute to a hierarchical process that begins with initial cell contact and ends with functional pre- and postsynaptic structures (Ziv and Garner, 2001).

Narp is a neuronal immediate early gene (IEG) and is a member of the pentraxin family (Tsui et al., 1996). Pentraxins are secreted proteins that are understood to play roles in diverse processes ranging from the humoral immune response to nervous system development (Gewurz et al., 1995). Like other pentraxins, Narp is a secreted, calcium-dependent lectin (Tsui et al., 1996). Narp protein localizes specifically to excitatory synapses in primary neuronal cultures and in adult brain and is present in both the pre- and postsynaptic compartments (O'Brien et al., 1999). Narp specifically coclusters AMPA-type glutamate receptors (AMPARs) and does so when expressed either in the same cell or in a contacting cell (O'Brien et al., 1999). When Narp transgene is expressed in cultured spinal neurons, it increases the number of dendritic AMPAR clusters (O'Brien et al., 1999), and dominant-negative Narp reduces the number of AMPAR clusters (O'Brien et al., 2002). These studies define Narp to be an essential synaptogenic factor that is specific for excitatory synapses.

Unlike many other synaptogenic factors, Narp is expressed as an IEG (Tsui et al., 1996). IEGs mediate protein synthesis-dependent cellular adaptation and are essential for long-term synaptic plasticity (Kandel, 2001). In the present study, we demonstrate that Narp is cofunctional with another neuronal pentraxin termed NP1 (Schlimgen et al., 1995). We demonstrate that NP1 is a synaptic protein and is physically linked to Narp in a SDS-resistant complex. Studies from heterologous cells indicate that Narp and NP1 coassemble into a highly ordered quaternary structure that is maintained by specific disulfide bonds between oligomers. The composition of the pentraxin complex is important for its function. Compared to Narp, NP1 shows a modest ability to induce excitatory synapse formation in neurons. However, when the pentraxins are coexpressed, their synaptogenic activity can be greater than either alone. A molecular model is evinced in which Narp coassembles with NP1 and confers distinct clustering activity upon the pentraxin complex. Since Narp is dynamically regulated by activity and rapidly integrated into a mixed pentraxin complex with NP1, neurons can create a continuous palette of synaptogenic agents that are tuned for the developmental state or activity history.

Results

NP1 and Narp Colocalize at Excitatory Synapses

Like Narp, NP1 is primarily expressed in the nervous system and is a bimodular protein, with an N-terminal half that is predicted to form coiled coils and a C-terminal half that encodes a pentraxin domain (Hsu and Perin, 1995; Schlimgen et al., 1995; Tsui et al., 1996). The pentraxin domain of Narp is 65% identical to NP1, while the coiled-coil domain is 42% identical. Using pen-

*Correspondence: pworley@jhmi.edu
[4]These authors contributed equally to this work.
[5]Present address: Cellzome AG, Meyerhofstrasse 1, 69117 Heidelberg, Germany.

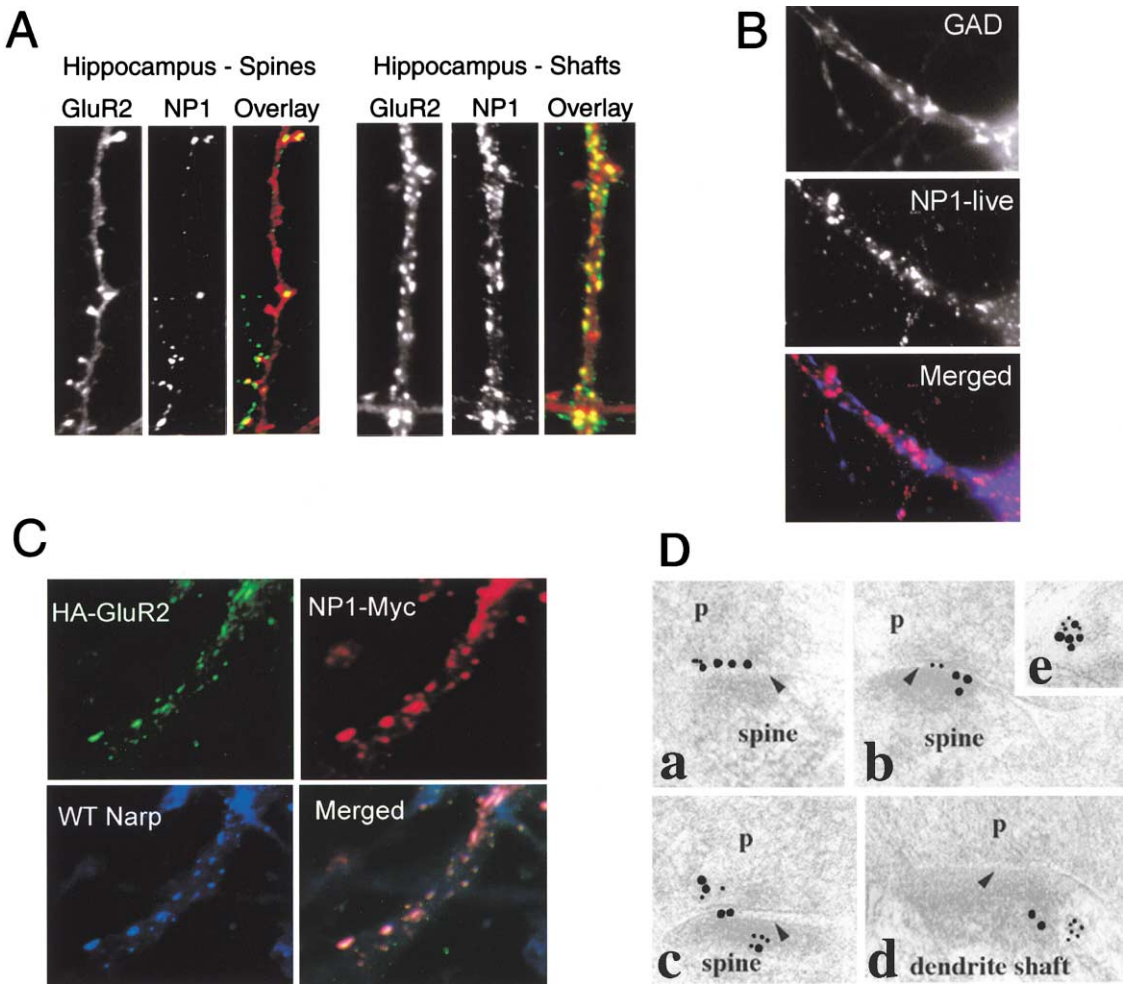

Figure 1. NP1 Is Enriched at Excitatory Synapses and Associates with Narp and AMPA Receptors

(A) NP1 and GluR2 colocalize on dendritic spines and shafts. Hippocampal neurons on day 17 in vitro were stained with anti-NP1 and anti-GluR2 antibodies following fixation and permeabilization.

(B) NP1 is not present at inhibitory synapses. Lack of overlap of NP1 visualized on live neurons and glutamic acid decarboxylase (GAD) detected after fixation and permeabilization on a hippocampal neuron at day 16.

(C) Narp, NP1, and GluR2 colocalize at hippocampal dendrites. E18 hippocampal neurons were transfected after 17 days in vitro and stained 48 hr later with anti-HA, anti-Narp, and anti-*myc* antibodies following fixation and permeabilization.

(D) NP1 colocalizes with Narp at excitatory synapses in adult brain. Double-immunogold labeling for NP1 (5 nm) and Narp (10 nm) in the rat hippocampus ([Da] molecular layer of dentate gyrus; [Db] and [De] CA1 stratum oriens; [Dc] hilus) and cerebral cortex ([Dd] layer 1). (Da) NP1 (three gold particles) and Narp (four gold particles) line up along the presynaptic side of a spine synapse. (Db) Narp and NP1 at spine synapse in CA1 stratum oriens. (Dc) Note the colocalization of NP1 and Narp in presynaptic and postsynaptic clusters. (Dd) Narp and NP1 at a dendritic shaft synapse where Narp appears to associate with a vesicle. (De) Narp and NP1 colocalize to vesicle-like structure in an unidentified process in the neuropil. Line scale is 0.1 μm.

traxin-selective antisera, we examined the distribution of native NP1 in primary neuronal cultures (Figure 1). The immunocytochemical distribution of NP1 in cultured hippocampal neurons reveals similarities with the previously described distribution of Narp (O'Brien et al., 1999). Like Narp, NP1 is present in the somatodendritic compartment of aspiny neurons, which presumably represent inhibitory interneurons (Craig et al., 1994). NP1 is enriched in large clusters that almost entirely colocalized with GluR2 aggregates (Figure 1A), a marker for excitatory synapses (Mammen et al., 1997; O'Brien et al., 1997). Whereas Narp is absent from synaptic spines in cultured neurons (O'Brien et al., 1999), NP1 and GluR2 colocalize on some spines. A clustered distribution of NP1 on the cell surface is revealed when the NP1 antibody is applied to live neurons prior to fixation. Surface clusters of NP1 do not colocalize with glutamic acid decarboxylase (GAD), a marker for inhibitory axons (Figure 1B).

We next examined targeting of Narp, NP1, and GluR2 transgenes expressed in primary hippocampal neurons (Figure 1C). E18 hippocampal cultures were transfected at 10 DIV and examined by live staining after an additional 2 days. Figure 1C shows the high degree of colocalization of these proteins in dendrites. We conclude that both native and transgene NP1 and Narp target selectively to excitatory synapses.

To assess the extent colocalization of Narp and NP1, we examined their distribution using double immunoEM

in brain. NP1 and Narp gold particles, 5 nm and 10 nm, respectively, are predominantly present over presynaptic elements and the synaptic cleft in fiber terminals in CA3 stratum lucidum and hilus of the rat hippocampus (Figure 1D). Mossy fiber synapses in the hippocampal hilus show colocalization of Narp and NP1 in the same presynaptic compartment where labeling is absent from the main mass of synaptic vesicles. Instead, it is present near the presynaptic plasma membrane or over electron-dense vesicular structures. One such vesicular profile is shown in Figure 1De, labeled intensely for both Narp and NP1. NP1 and Narp gold particles are also present at synapses onto dendritic shafts or short spines of neurons with the morphological resemblance of inhibitory interneurons. Narp and NP1 colocalize at synapses in all forebrain regions examined including the statum oriens of CA1 and layers 1 and 5 of the neocortex (data not shown). These studies confirm that NP1 and Narp colocalize at excitatory synapses in vivo and are present in both pre- and postsynaptic compartments.

Narp and NP1 Form Redox-Dependent, SDS-Stable Multimers that Require the N Terminus

We examined the biophysical properties of Narp and NP1 that are essential for their action at the synapse. Narp cDNA encodes a 432 amino acid protein with an N-terminal signal sequence (predicted 16 aa), followed by two coiled-coil domains (~41–89 and 103–206 of mature protein) and a C-terminal pentraxin domain (Tsui et al., 1996) (Figure 2A). Coils (Lupas et al., 1991) predict the second coiled-coil domain to be composed of three contiguous coils. NP1 possesses a similar domain structure (Figure 2A). Immunoblot of brain extract prepared with 2% SDS and β-mercaptoethanol (BME) reveals a single band with the predicted molecular weight of ~50 kDa (Figure 2B). An identical pattern sensitive to BME is observed for NP1. If extracts from either brain or HEK 293 cells are not treated with reducing agent, Narp migrates as a complex of bands >250 kDa. These observations suggest that mature Narp and NP1 in brain, and transgene Narp from HEK 293 cells, are disulfide-linked proteins.

To assess whether the high-molecular species might be due to disulfide linkage of Narp to another protein, we purified Narp from HEK 293 cells using immunoaffinity chromatography and performed SDS-PAGE. Native and reduced proteins were visualized by silver stain (Figure 2C). In nonreducing conditions, silver stain reveals a single broad protein band of >250 kDa. The same material migrates as a single band of 50 kDa after treatment with reducing agent. Bands were confirmed to be Narp by Western blot. Importantly, no additional bands were detected by silver stain, indicating that the high-molecular weight (mw) species is either a homomultimer, or Narp linked to another protein of similar size. In further confirmation of the homomultimer hypothesis, treatment with endoglycosidase H and reducing agent results in a single band that migrates ~45 kDa (data not shown). We conclude that the >250 kDa species expressed in HEK 293 cells represents Narp homomultimer.

Pentraxin family members are known to self-associate into multimers of 5 to 12 subunits (Emsley et al., 1994; Gewurz et al., 1995). For several pentraxins, disulfide linkages between pentraxin domains stabilize the multimers. Narp encodes seven cysteines: three in the N-terminal half and four in the C-terminal half (Figure 2A). In the N terminus, the first two cysteines precede the first coiled-coil domain; the third cysteine is within the first coiled-coil domain. The cysteines in the C-terminal half are widely distributed within the pentraxin domain. We generated and tested deletion mutants that retained either the pentraxin domain or the N-terminal half to determine their respective contributions to the reducing agent-dependent shift in mw (Figure 2D). When expressed in HEK 293 cells, the N-terminal construct [Narp (Δ191–410)] forms high-molecular weight bands that shift to monomers upon reduction. By contrast, the pentraxin domain alone [Narp (Δ12–196)] behaves as a monomer in either reducing or nonreducing conditions. This analysis suggests that cysteines in the N-terminal half of Narp are important for multimer formation.

Cysteines within the N Terminus Are Essential for Narp Multimerization

To test the role of specific N-terminal cysteines (C14, C26, and C79) in multimer formation, we generated a series of point mutants in which individual cysteines were replaced with serine. wt Narp and Narp mutant proteins were expressed in HEK 293 cells. Secreted Narp present in conditioned medium was immunoprecipitated with Myc antibody and analyzed by Western blot without reducing agent (Figure 2E). Narp (C14S) migrates as three distinct species with apparent mws of 100, ~200, and >250 kDa, consistent with dimer, tetramer, and pentamer/hexamer, respectively (lane 3). Narp (C26S) shows bands of similar mw and additionally includes a higher mw band (lane 4). The similarity of the pattern suggests that C14 and C26 make similar contributions to multimer assembly. By contrast, Narp (C79S) produces a single, broad band of >250 kDa (lane 5). The absence of dimers or tetramers with the Narp (C79S) indicates that C14 and C26, which are retained in Narp (C79S), bind to distinct Narp molecules. It is important to note that the largest mw bands of the Narp cysteine point mutants are of distinctly lower apparent mw than the broad, uppermost band of wild-type Narp.

Double-cysteine mutants confirmed the role of all individual N-terminal cysteines in multimer formation. Narp (C14,26S) (only C79 present) migrates as a predominant dimer and a monomer (lane 6). Narp (C14,79S) and Narp (C26,79S) also migrate as dimers (lanes 7 and 8). The triple mutant Narp (C14,26,79S) migrates as a single band that is identical in size to wild-type Narp protein treated with reducing agent (lane 9 versus lane 2). Thus, all the cysteines in the N terminus are involved in intermolecular disulfide linkage and are necessary and sufficient for formation of SDS-stable, high-molecular weight species.

Cysteine-dependent complexes were examined by negative-staining transmission electron microscopy. Narp proteins were purified by Myc affinity chromatography and eluted in pH 4.0 acetate buffer. Proteins remained stable in solution at pH 4.0 but rapidly precipitated when buffered to pH 7.4 in PBS. wt Narp was deposited on the grid ~2 min after titration to pH 7.4,

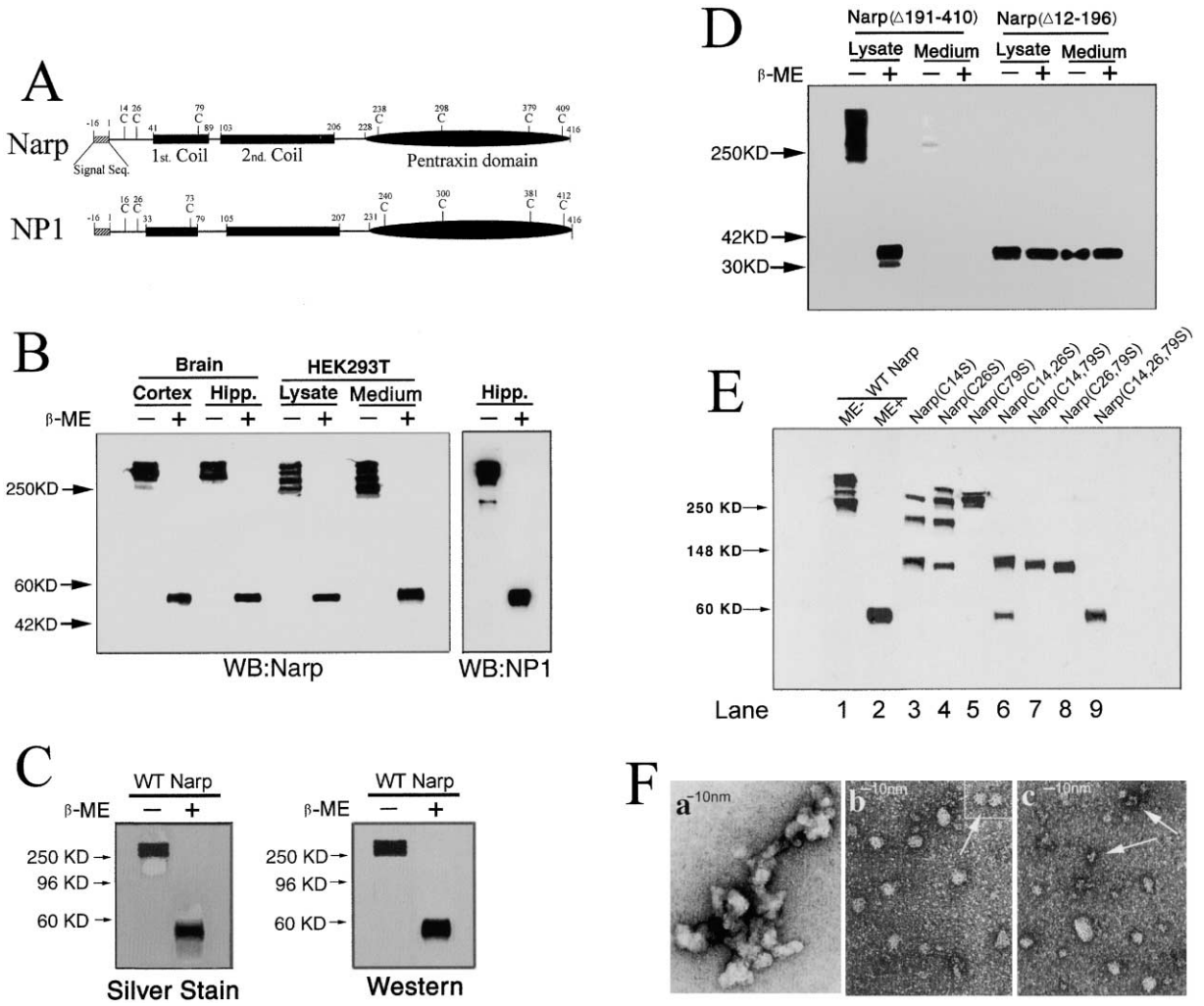

Figure 2. Cysteines in Narp N Terminus Contribute to Narp Polymerization

(A) Diagram of Narp and NP1 domain structure and cysteine distribution.

(B) Immunoblot of Narp and NP1 from adult rat brain (cortex and hippocampus) and from transfected HEK 293 cells prepared with or without reducing reagent (BME). In nonreducing conditions, Narp and NP1 migrate with an apparent molecular mass >250 kDa. Narp and NP1 treated with BME migrate at ~50 kDa, the predicted monomer size.

(C) Myc-tagged Narp was expressed in HEK 293 cells and IPed from culture medium using a monoclonal Myc antibody. Narp migrates as a single band of >250 kDa in a silver-stained gel without reducing agent and ~50 kDa when treated with BME. Narp immunoblot confirms the identity of the protein bands.

(D) Immunoblot of Narp (Δ191–410) and Narp (Δ12–196) samples which have been prepared from HEK 293 cells with and without BME indicates cysteines in Narp N terminus are involved in Narp polymerization. See Results for details.

(E) Myc-tagged Narp point mutants of N-terminal cysteines were IPed from culture media of transfected HEK 293 cells. Samples were then analyzed under nonreducing conditions by gradient (4%–20%) SDS-PAGE. Immunoblots were analyzed using Narp antibody. See Results for descriptions.

(F) EM negative stain images of purified Myc-tagged Narp and Narp mutants. (Fa) wt Narp appears as a large complex of aggregated globules. (Fb) Narp (C79S) (preparation of lane 5 of blot in Figure 2E) appears as compact and regular globular structures of ~12 nm diameter. Occasional paired structures were detected (arrow). (Fc) Narp (C26S) (preparation of lane 4 of blot in Figure 2E) shows complexes of different sizes, consistent with dimers (arrow), tetramers, hexamers, and higher-order multimers. See Results for further description.

at which time the solution remained free of visible precipitate. EM of this material demonstrates that Narp aggregates in large, irregular clusters that do not reveal a discrete modularity (Figure 2Fa). We next examined Narp (C79S), which in Figure 2E (lane 5) forms a predominant single hexameric species. Narp (C79S) also precipitates upon titration to pH 7.4, so to visualize the soluble units, grids of the pH 4 material were prepared. EM reveals that Narp (C79S) is a relatively uniform, globular structure of ~12 nm diameter (Figure 2Fb). This is consistent with the predicted size of a Narp hexamer based on the crystallographically defined size of pentraxins C-rp/SAP, which is ~5 nm/monomer (Emsley et al., 1994; Shrive et al., 1996). While isolated Narp (C79S) globules predominate in the EM field, many examples of paired globules are detected (Figure 2Fb, inset). For comparison purposes, we next examined Narp (C26S), which migrates in SDS-PAGE as dimer, tetramer, and

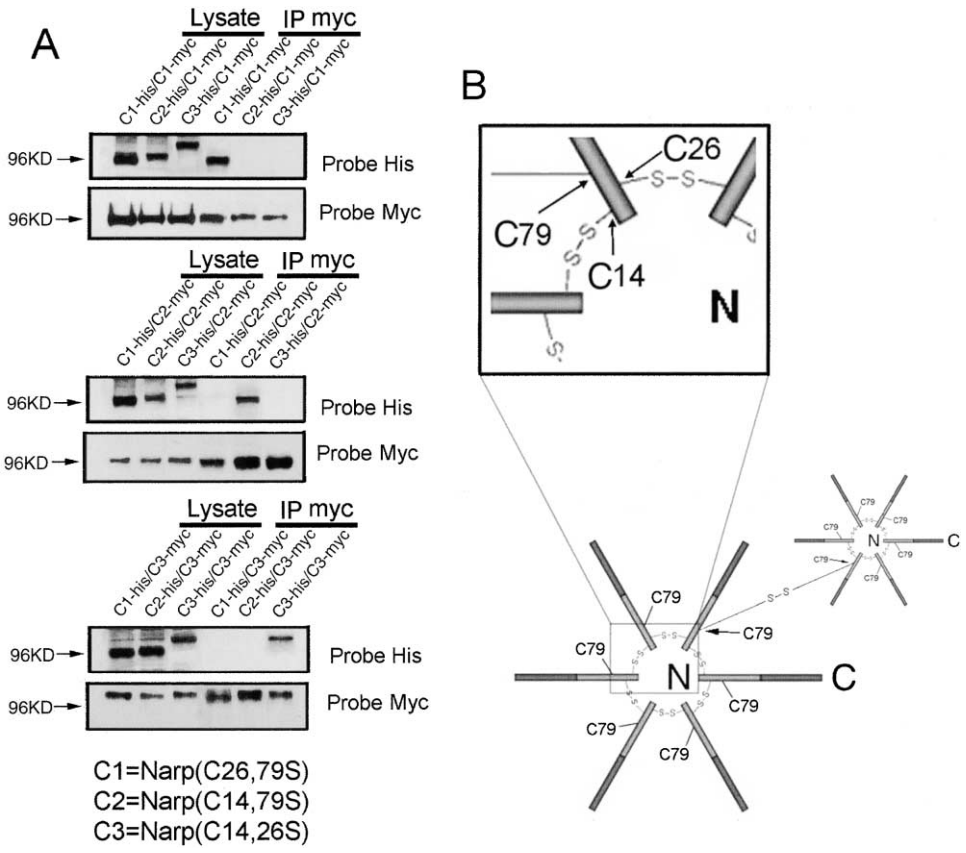

Figure 3. Position-Specific Disulfide Linkages between Narp Subunits

(A) Myc-tagged and His-tagged double cysteine Narp mutants were cotransfected into HEK 293 cells. Myc-tagged Narp was IPed with monoclonal anti-*myc*, and noncovalently linked His-tagged Narp was washed away with 0.5% SDS and 0.5 M NaCl. Samples were immunoblotted with polyclonal anti-His and anti-*myc*. All Narp mutants migrate as dimers as in Figure 2E (lanes 6–8). CoIP with Myc-tagged Narp was dependent on the position of the remaining cysteine. C1-*myc* coIPs only C1-His, C2-*myc* coIPs only C2-His, and C3-*myc* coIPs only C3-His. [C1 = Narp (C26,79S); C2 = Narp (C14,79S); C3 = Narp (C14,26S)].

(B) Model of intermolecular disulfide linkages between C14s and C26s that form the "core" Narp hexamer structure. C79 is modeled to bridge between hexamers.

hexamer (Figure 2E, lane 4). EM grids were again collected at pH 4 and EM of this material reveals a mixture of structures that included 12 nm globules as well as smaller profiles consistent with tetramers and/or dimers (Figure 2Fc). Since EM images were obtained under conditions that could denature protein-protein interactions (pH 4), we use them to reveal only the cysteine-dependent multimer state. The concordance of the EM observations with the behavior of the Narp proteins in SDS-PAGE suggests that EM profiles represent the basic units of disulfide-linked Narp assembly.

Cysteines Form Position-Specific Intermolecular Disulfide Linkages

To examine the specificity of disulfide linkages, we coexpressed His-tagged and Myc-tagged Narp mutants that retained one of the three cysteines and assayed for dimer formation by coIP (Figure 3A). We determined that 0.25% SDS (see Figure 4D) in pH 7.4 PBS dissociates Narp monomers that are not associated by disulfide linkage (see also Figure 4D). Myc-tagged Narp (C26,79S) coIPs His-tagged Narp (C26,79S) but not the other double mutants Narp (C14,79S) or Narp (C14,26S), which retain only the second or third cysteine. Similarly, Myc-tagged Narp (C14,79S) coIPs His-Narp (C14,79S) but not Narp (C26,79S) or Narp (C14,26S). Finally, Myc-tagged Narp (C14,26S) coIPs His-Narp (C14,26S) but not Narp (C26,79S) or Narp (C14,79S). Thus, Narp monomers are linked to other Narp monomers by intermolecular disulfide bonds that form between cysteines at identical positions in their N termini. This observation indicates that interactions between the N termini are highly ordered, since only identically positioned cysteines are capable of covalent bonding.

Findings presented in Figures 2 and 3 support a model for assembly of Narp monomers into disulfide-linked hexamers by position-specific intermolecular bonds at C14 and C26 (Figure 3B). Our model envisions a ring based on precedent from crystallographically resolved short pentraxins (Gewurz et al., 1995). Since mutation of C79 does not result in formation of dimers or tetramers, we model C14 and C26 to bind neighboring Narp monomers to form a hexamer ring. C14 and C26 share the property that they precede the first predicted coiled-coil domain. C79, which is at the C terminus of the first coiled coil, is modeled to disulfide bond between distinct

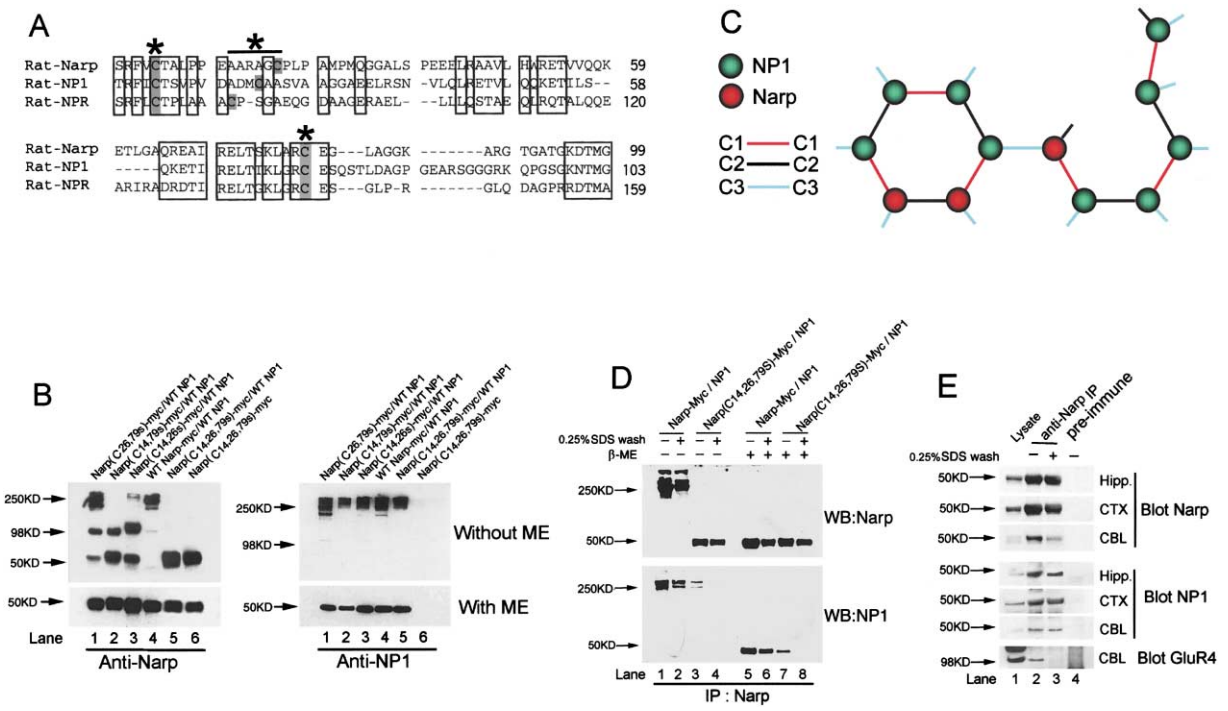

Figure 4. Narp and NP1 Form Heteromultimers via N-Terminal Protein-Protein and Specific Intermolecular Disulfide Interactions

(A) Alignment of cysteines (*) in Narp, NP1, and NPR (see Discussion). The positions of the first and the third cysteines in N terminus are conserved. The second cysteine is distinctly positioned in each of the pentraxins.

(B) CoIP analysis of wt NP1 with Narp cysteine mutants and deletion mutants of Narp. HEK 293 cells were transfected with Narp and NP1 constructs, and proteins were IPed from medium with Myc Ab in conditions that maintain protein-protein interactions (1% Triton X-100/PBS). Samples prepared with or without reducing agent were analyzed by immunoblotting.

(C) Molecular model of NP1-Narp intermolecular disulfide linkages that mediate heteromultimer formation. The C2-C2 disulfide linkage is modeled to be pentraxin specific. The model predicts that pairs of Narp may coassemble with pentraxins or that the mixed assembly may not be fully crosslinked.

(D) Narp-NP1 protein-protein interactions but not disulfide linkage mediated interactions are dissociated by a 0.25% SDS wash.

(E) Narp and NP1 coimmunoprecipitate in a SDS stable complex. Narp was IPed with goat anti-Narp from hippocampus (Hipp), cortex (CTX), and cerebellum (CBL). NP1 coIPed with Narp from all tested tissues. The interaction between Narp and NP1 can not be disrupted by a 0.25% SDS wash. By contrast, the interaction between Narp and GluR4 was dissociated by 0.25% SDS wash.

hexamers. Since the largest SDS-stable Narp species from HEK 293 cells or brain are of discrete size (smaller than ryanodine receptor, for example), our model suggests that not all C79 are involved in intermolecular linkages. Of additional note, we consistently see that the C3 Narp-mutant dimer (mediated by C79) runs with a larger apparent mw than C1 or C2 Narp yet runs with the same size after BME (Figure 3A). Based on this and other observations, it is possible that an additional protein is present in the complex, perhaps as a bridge at C3. Efforts to identify this putative protein are ongoing.

Narp Forms Heteromultimers with NP-1 that Require the N Terminus and Involve Both Disulfide Linkage and Protein-Protein Interactions

Narp and NP1 show similar redox-dependent electrophoretic mobility (Figure 2B) and cofractionate from brain (Kirkpatrick et al., 2000). NP1 encodes cysteines at positions 16, 26, and 73, which are nearly identical to the positions of cysteines in Narp (Figure 4A). Since these cysteines mediate covalent assembly of Narp complexes, we examined the possibility that the equivalent cysteines of NP1 mediate disulfide interactions that covalently link Narp and NP1 into mixed complexes.

wt NP1 was coexpressed with Myc-tagged wt Narp or Narp cysteine point mutants, and their interaction was assayed by IP with Myc Ab (pulls down Narp) followed by Western blot for Narp and NP1. To assess interactions mediated by protein-protein versus disulfide linkage, SDS-PAGE was performed on samples that were prepared in 1% Triton either with or without reducing agent. wt NP1 coIPs with wt Narp (Figure 4B; right blot; lane 4). In a manner identical to Narp, the coIPed NP1 runs as a high mw multimer (>250 kDa) in the absence of reducing agent and as a 50 kDa monomer when treated with BME. When coexpressed with wt Narp, the band pattern of the coIPed NP1 is identical to that detected by Narp Ab (Figure 4B; compare right and left blots; lane 4), consistent with the notion that the proteins were part of the same complexes.

NP1 also coIPs with Narp (C26,79S) (retains only C14) and the majority of NP1 migrates as a >250 kDa species (Figure 4B; right blot; lane 1). In this same extract, Narp (C26,79S) displays a more complex pattern with monomer, dimer, and a >250 kDa species, all of which reduces to 50 kDa with BME treatment (left blot; lane 1). The dimer band is consistent with a NarpC14-NarpC14 disulfide linkage as was observed when Narp (C26,79S)

is expressed alone (Figure 2E; lane 8). The putative dimer band is not the result of linkage to NP1, since there is no NP1 at this mw (compare Figure 8, lane 1 of Narp/NP1 blots). In contrast to the band pattern of Narp (26,79S) when expressed alone (Figure 2E; lane 8), when Narp (C26,79S) is coexpressed with NP1, it also appears as a >250 kDa species (Figure 4B; lane 1). This species is inferred to be Narp (C26,79S) covalently linked to wt NP1. NP1 also coIPs with Narp (C14,79) (retains only C26) (Figure 4B; right blot; lane 2). In contrast to Narp (C26,79S), Narp (C14,79) migrates as a monomer and dimer but did not appear in the >250 kDa complex. This pattern indicates that C26 of Narp is available to form disulfide linkage to other Narp monomers but does not effectively link to NP1. Narp (C14,26S) (retains only C79) reiterates these points. Narp (C14,26S) coIPs NP1 and NP1 migrates >250 kDa (Figure 4B; right blot; lane3). Blotting the same precipitates with anti-Narp antibody, the Narp (C14,26S) pattern indicates a predominance of Narp-Narp dimers and infrequent incorporation into NP1 multimers at >250 kDa (Figure 4B; left blot; lane 3). Therefore, Narp-NP1 assemblies involve disulfide linkages with Narp C14, less so by C79, and not by C26. While these studies were performed on soluble proteins, the same rules for covalent assembly were confirmed for biotinylated surface proteins (data not shown).

Finally, NP1 coIPs with Narp (C14,26,79S) (Figure 4B; right blot; lane 5). In this result, all of the NP1 ran as >250 kDa species, while all the Narp migrates as monomer (left blot; lane 5). We conclude that the Narp and NP1 associate by protein-protein interactions that are robust even in the absence of disulfide linkage. This observation parallels the observation that Narp (C14,26,79S) can coIP wt Narp in the absence of disulfide linkage (data not shown). These interactions may be important for assembly of the complex prior to disulfide bond formation and may be important for the specificity of the disulfide linkages at each of the three cysteines.

These observations support a model (Figure 4C) of a mixed assembly composed of Narp and NP1 into disulfide linked multimers. The model highlights a preference for Narp/Narp or NP1/NP1 dimer formation at their respective C2 positions and is consistent with rules of homomeric and heteromeric assembly (Figures 2E and 4B).

Native NP1 and Narp Associate in a SDS-Stable Complex

To determine whether Narp and NP1 form covalently-linked heteromeric complexes in vivo, we used immunoprecipitation assays with detergent wash conditions that dissociate Narp-NP1 complexes not linked by disulfide bonds. When NP1 is coexpressed with a Narp point mutant [Narp (C14,26,79S)] that cannot form disulfide linkages with NP1, the proteins coimmunoprecipitate if cell lysates are solubilized with 1% Triton X-100 in PBS and washed in the same lysis buffer but do not coIP if washed with 0.25% SDS in PBS (Figure 4D). In contrast, if wt Narp and NP1 are coexpressed, they coIP even with 0.25% SDS wash. The pentraxin complex runs on nonreducing SDS page as a >250 kDa complex. When the same precipitates are treated with reducing agent prior to SDS-PAGE, they migrate as ~50 kDa monomer species. To test the detergent and reducing agent-dependent association of Narp and NP1 in brain, we performed coIP experiments from rat cortex, hippocampus, and cerebellum. Soluble lysates were prepared in PBS with 1% Triton X-100 and IPed with goat antibody specific for Narp. IPs were then washed with either 1% Triton/PBS or 0.25% SDS/PBS and analyzed by SDS-PAGE in reducing conditions. CoIP assays using Triton X-100 confirmed that antibody specific for Narp coIPed NP1 (Figure 4E). This association was also confirmed by showing that rabbit antibody specific for NP1 coIPs Narp (see Figure 6A). When IPs are washed with 0.25% SDS, Narp antibody retains the ability to coIP NP1. As a control for the stringency of SDS wash, we confirm that GluR4, which coIPs with Narp from cerebellum using Triton X-100 wash, is dissociated by 0.25% SDS wash. We conclude that Narp and NP1 are physically associated in vivo in a complex that is resistant to SDS and likely involves disulfide linkages.

The N Termini of NP1 and Narp Determine Their Distinct Surface Clustering Capability While Their Pentraxin Domain Mediates Interactions with GluRs

To examine the functional contribution of the N-terminal coiled-coil and C-terminal pentraxin domains of Narp and NP1, we engineered chimeric pentraxin molecules (Figure 5A). NP1/Narp consists of NP1's N-terminal half (aa 1–235) and Narp's C-terminal pentraxin domain (aa 234–432). Narp/NP1 features the inverse arrangement. In our initial characterization of these chimeric molecules, we coexpressed neuronal pentraxins and GluR2 in HEK 293 cells and performed coIP assays from cell lysates. Consistent with previous studies, GluR2 coIPs with Narp (Figure 5B; O'Brien et al., 1999). Similarly, NP1 and both chimeras are able to coIP GluR2 and are indistinguishable from wt Narp (Figure 5B). Interestingly, the isolated pentraxin domain of NP1 coIPs GluR2, whereas GluR2 does not coIP with the N-terminal half alone (Figure 5B; lanes 1 and 2). Consistent with the high degree of conservation between the pentraxin domains, the pentraxin domain of Narp coIPs GluR2 as well (data not shown).

To compare the propensity of the two neuronal pentraxins to form cell surface clusters, we transfected COS cells with Myc-tagged versions of the proteins. After 48 hr, the surface molecules of live cells were labeled with polyclonal anti-pentraxin antiserum. After fixation and permeabilization, the total cellular pool of pentraxin was stained with monoclonal anti-*myc* antibody. NP1 clusters appear smaller than Narp (Figure 5C). To provide an objective comparison, we determined the number of double label (cell surface) clusters of different sizes using Metamorph. The typical Narp clusters that we have described previously (O'Brien et al., 1999) are >50 pixels in these images. The number of clusters >50 pixels are 2.6-fold greater for Narp than for NP1 (30.7 ± 14.9/cell [n = 17 cells] versus 11.8 ± 9.6/cell [n = 11 cells]; $p < 0.05$; three independent transfections). For clusters >80 pixels, this ratio is even larger at 3.5 (Narp 17.2 ± 10.7 [n = 19 cells] versus NP1 4.9 ± 4.1 [n = 11 cells] clusters/cell; $p < 0.05$). By contrast, the number of clusters >10 pixels are comparable (NP1 89.6 ± 73 [n = 51 cells] versus Narp 99.7 ± 38.4 [n = 53 cells]). Thus, cells express-

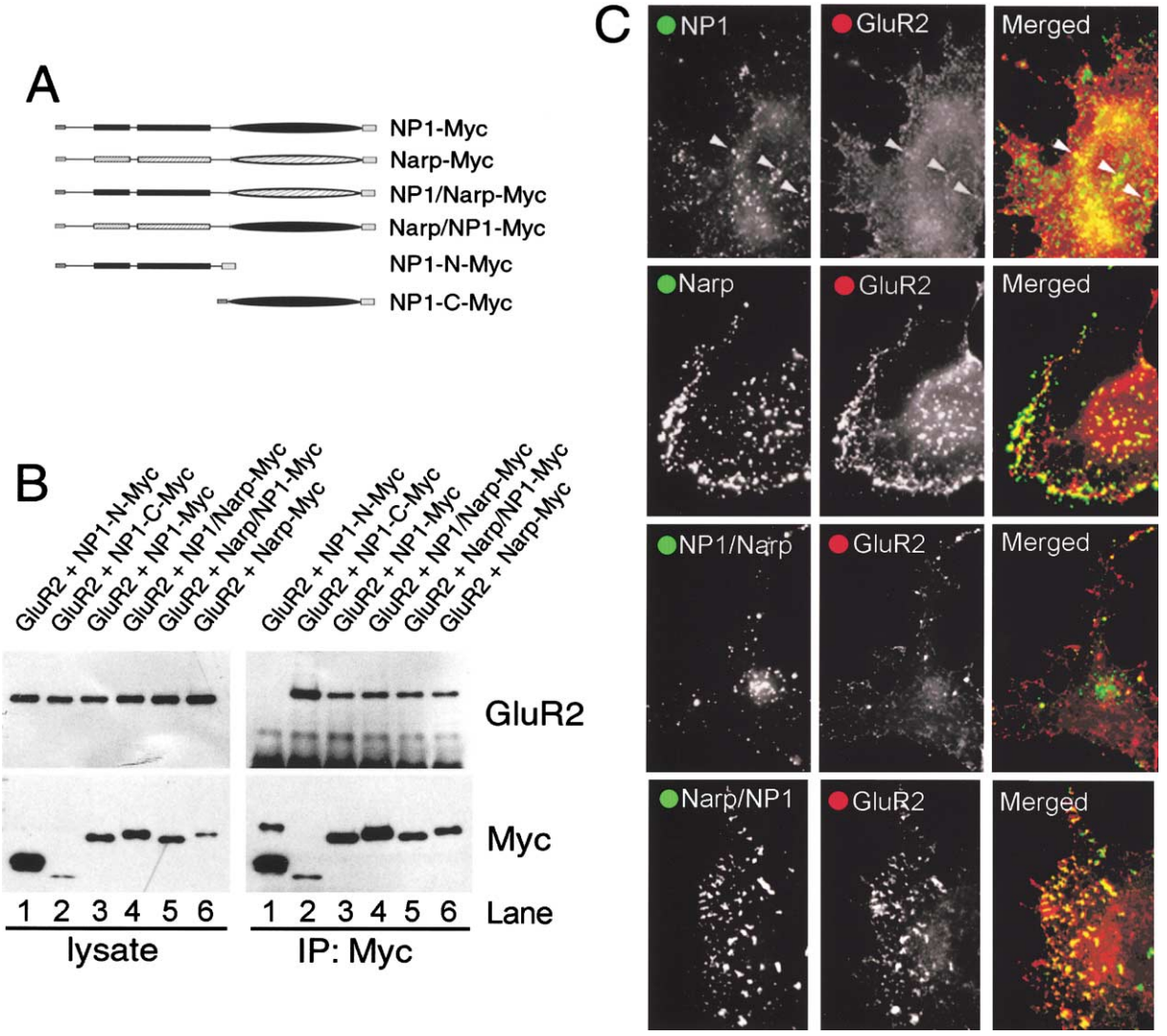

Figure 5. Narp and NP1 Show Distinct Clustering Properties that Are Dependent on Their N-Terminal Domains

(A) Schematic of pentraxin constructs employed in this study. In construct NP1-C-*myc*, the C-terminal half of the molecule comprising the pentraxin module was linked to the original signal peptide.

(B) Protein complexes in lysates of transfected cells were immunoprecipitated with anti-*myc* antibody and probed with GluR2 antibody. The pentraxin domain of NP1 is both required and sufficient for AMPA receptor binding (right blot; lanes 1 and 2). The degree of Narp/NP1 and NP1/Narp chimeric molecules binding to GluR2 is similar when compared to each other as well as to those of parental molecules.

(C) NP1 and Narp cocluster with AMPAR on the cell surface of transfected HEK 293 cells. NP1 clusters are smaller than Narp and are less effective in coclustering AMPAR. Narp/NP1-chimeric molecule displays Narp-like clustering and AMPA receptor coclustering activity, whereas the NP1/Narp chimera is NP1-like. See Results for description and quantitative analysis.

ing Narp and NP1 show similar numbers of clusters, but Narp-expressing cells show more large clusters.

To compare how AMPA receptors could be recruited into these surface aggregates, we coexpressed neuronal pentraxins and HA-tagged glutamate receptor subunits in COS cells and labeled both recombinant proteins in live cells with appropriate antibodies. NP1 is capable of recruiting the AMPA receptor subunit GluR2 into self-aggregates; however, the degree of colocalization between NP1 and GluR2 appear less than for Narp and GluR2 (Figure 5C). To gain an objective measure of pentraxin-induced coaggregation of glutamate receptors, we computed a colocalization index for GluR2 and each of the pentraxins. The score was normalized for Narp-GluR2 colocalization, which was set as 100%. The quantitative evaluation of 20 to 30 cotransfected cells confirms that NP1 is a less efficient clustering agent for GluR2 in heterologous cells than Narp (AMPAR colocalization with NP1 [71.0% $\pm$ 52%] versus with Narp [100.0% $\pm$ 39%]; $p < 0.001$). For both pentraxins, limited colocalization with GluR6 is measured (25.9% $\pm$ 13% for Narp; 23.0% $\pm$ 14% for NP1), values that represent random overlap between two labeled proteins in this assay. These assays indicate that NP1 is less effective in coclustering GluR2 than Narp.

We next examined the effect of swapping Narp and NP1 domains on their ability to form cell surface clusters. We first labeled surface chimeras alive with pentraxin

antibody and after fixation and permeabilization, labeled total cell pentraxin with anti-*myc* antibody. We then examined the size of double-labeled clusters. Narp/NP1 clusters are significantly larger than those of NP1/Narp (Figure 5C). The number of clusters >50 pixels are 2-fold greater for Narp/NP1 than for NP1/Narp (26.6 ± 10.2/cell [n = 19] versus 13.8 ± 13.6/cell [n = 11]; $p < 0.01$). Both chimeras cocluster GluR2HA (Figure 5C) but not GluR6HA (data not shown). Using the normalized (to wt Narp) colocalization assay, Narp/NP1 is more efficient coclustering GluR2 than NP1/Narp (65.9 ± 20.7 [n = 20 cells] versus 36.3 ± 16.8 [n = 26 cells]; $p < 0.0001$) confirming the interpretation that Narp/NP1 is a Narp-like molecule, whereas NP1/Narp is NP1-like. We conclude that the N termini of Narp and NP1 confer distinctive properties that are manifest in the size of surface clusters and their ability to cocluster GluR2 on heterologous cells.

NP1 and Narp Are Differentially Regulated and Form Complexes that Are Dynamically Altered by Activity

We sought to define mechanisms that regulate the composition of the pentraxin complex in brain. Many members of the pentraxin family are rapidly induced by tissue-specific stimuli (Gewurz et al., 1995). For example, Narp expression is rapidly upregulated following seizure (O'Brien et al., 1999). Therefore, we examined the possibility that intense neuronal activation might alter NP1 expression. In addition, we examined the possibility that newly synthesized Narp becomes associated with NP1.

Maximal electroconvulsive seizure (MECS) is a robust stimulus of IEG expression and was used in the original cloning of Narp (Tsui et al., 1996). MECS-stimulated rats were sacrificed at various times, and hippocampus was assayed for Narp and NP1. As reported previously (O'Brien et al., 1999), Narp protein increases by 3 hr and shows a peak induction between 6 and 12 hr (Figure 6A). The MECS-induced increase in Narp at 3 hr is blocked by pretreatment of the rat with the protein synthesis inhibitor cycloheximide, consistent with its rapid translation following mRNA induction (Tsui et al., 1996). By contrast, NP1 expression did not change after MECS and is not sensitive to cycloheximide. NP1 mRNA is also not changed following MECS (data not shown). We conclude that while Narp is rapidly upregulated by neuronal activity, NP1 is constitutively expressed and is not dynamically responsive to activity in the adult brain.

We next examined the composition of the Narp-NP1 complex as a function of neuronal activity. NP1 was immunoprecipitated using chicken anti-NP1 from detergent extracts of hippocampus prepared from a time course after MECS, and these precipitates were assayed for coIP of Narp (Figure 6A). The amount of Narp that coIPs with a constant amount of NP1 increases over time as a consequence of synaptic activation, and the time course of increased Narp coIP parallels the time course of Narp induction. This result indicates that Narp and NP1 become rapidly associated in vivo after de novo Narp synthesis.

We next examined the comparative levels of Narp and NP1 protein in brain. This issue is important for a model of mixed coassembly, as suggested in Figure 4C. The sensitivity of protein detection with Narp- and NP1-specific Abs was calibrated using a Myc Ab to detect identically tagged recombinant Myc Narp and NP1. We determined a dilution of transgene protein that corresponded to the amount of native Narp in control adult hippocampus and set this as one unit (U). Dilution standards from 0.1 U to 5 U were run with the tissue samples. To study expression levels in adult animals, we sacrificed rats 3 hr or 15 hr after MECS, as well as untreated controls. Cerebella, hippocampi, cortices, and brainstems were prepared, lysed, and together with calibrated pentraxin standards, analyzed by Western blotting with Narp and NP1 antibodies (Figure 6B). In this assay, we did not detect Narp in cerebellum, even with the longest exposures, indicating a level of Narp <0.1 units (U). In contrast, 5 U of NP1 is present in the same sample, indicating an excess of NP1 over Narp of at least 50-fold. In brainstem samples, ~2 U of NP1 is present, as opposed to ~0.2 U of Narp in control brain and ~0.6 U 15 hr after seizure. In hippocampus, a constant amount of ~6 U of NP1 is found with ~1 U Narp in control hippocampus and ~4 U Narp 15 hr after MECS. In cortex, NP1 is ~20 U in both control and MECS cortex while the relative amount of Narp is ~5 U in untreated animals and ~20 U 15 hr after MECS. We conclude that in naive adult rat brain, there is an excess of NP1 over Narp that ranges from 4-fold (cortex) to greater than 50-fold (cerebellum). MECS causes a 3- to 4-fold increase in Narp protein in all forebrain areas examined, thus equalizing pentraxin levels in cortex and hippocampus.

Observations from the adult brain indicate that NP1 is constitutively expressed. We sought to identify conditions during which NP1 levels might be regulated by examining postnatal development. We harvested hippocampi from rats at various time points during postnatal development and compared expression levels of Narp, NP1, and GluR1 by Western blotting (Figure 6C). Consistent with a previous report (Zhu et al., 2000), levels of the AMPA receptor subunit GluR1 increase steadily until the second week after birth and remain constant thereafter. Similarly, Narp protein levels are found to be low at the time of birth and peak at around 7 weeks of age. In contrast, expression of NP1 is very high during early postnatal development and declines dramatically between postnatal days 6 and 11. The Western blot in Figure 6C is exposed to illustrate NP1 developmental change and underrepresents the substantial levels of NP1 in the adult brain (Figure 6C). Based on our semiquantitative analysis of pentraxin levels, we estimate that NP1 is at least 100 times more abundant than Narp in P1 rat pup hippocampus.

To provide an anatomic correlate of the rapid biochemical coassociation of Narp and NP1 after MECS, we performed immunohistochemistry on rat hippocampus. Consistent with immunoEM results, NP1 expression is enriched in the CA3 region of the hippocampus in a distribution consistent with mossy fibers (Figure 6D). This localization is not dramatically altered by MECS. By contrast, double labeling of Narp illustrates a dramatic increase in immunoreactivity 16 hr following MECS that colocalizes with NP1. Since MECS induces Narp in granule cells (Tsui et al., 1996; O'Brien et al., 1999), these observations support a model in which Narp is rapidly

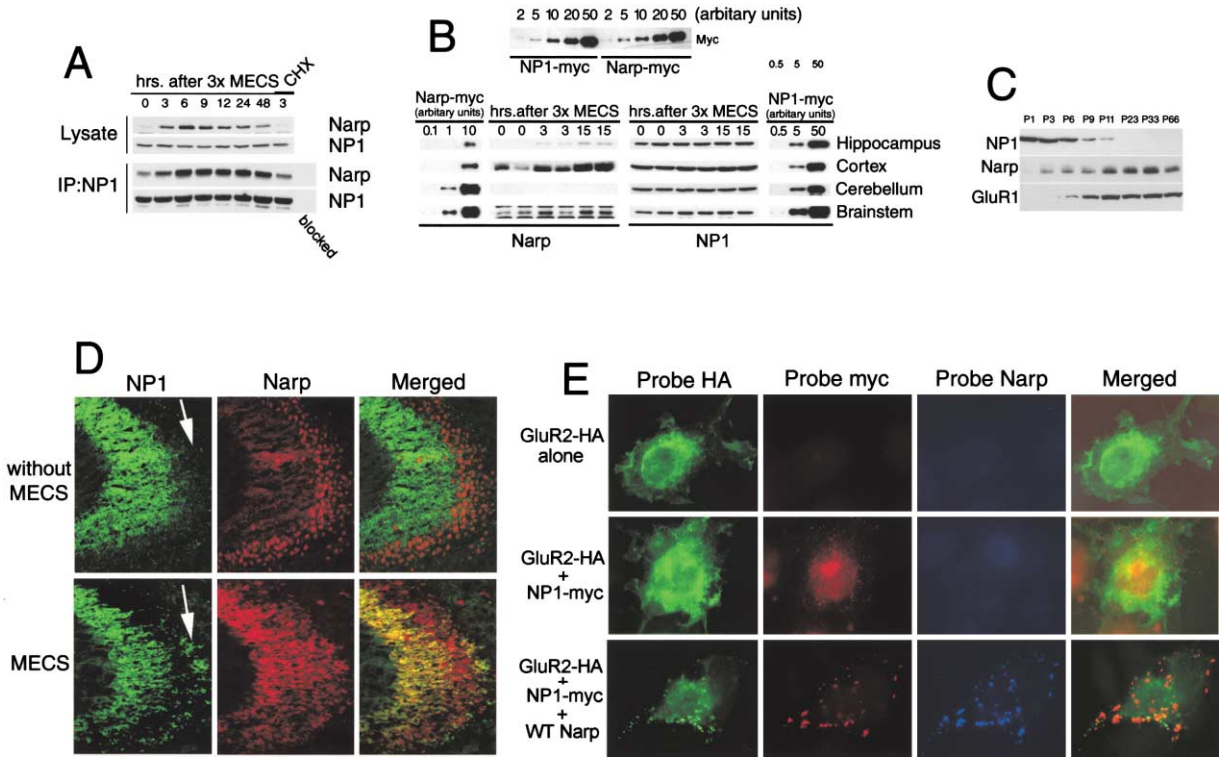

Figure 6. Narp and NP1 Are Differentially Regulated In Vivo, and Narp Expression Increases the Size of NP1 Surface Coclusters with GluR2

(A) NP1-Narp complex composition changes in an activity-dependent manner. Immunocomplexes were probed with pentraxin antibodies. Note the consistent IP of NP1 from all time points and the time-dependent increase in Narp that coIPs with NP1.

(B) Ratios of Narp and NP1 differ between brain areas, and they are altered in response to synaptic activity. Tissues prepared in duplicates. See Results for further description.

(C) Western blot analysis of developmental changes in NP1, Narp, and GluR1 expression in rat hippocampus.

(D) Narp is induced in mossy fiber terminals after MECS. In the upper panel showing hippocampus of naive rats, NP1 is predominantly expressed in CA3 neuron cell bodies and the mossy fiber terminal field, while Narp is abundant only in CA3 neurons. MECS induces Narp in mossy fiber terminal fields.

(E) The incorporation of Narp into NP1-GluR2 clusters increases cluster size. Cos cells were transfected with GluR2-HA, GluR2-HA/NP1-Myc, or GluR2-HA/NP1-Myc/wt Narp. The transfected cells were stained with rat anti-HA, mouse anti-*myc*, and rabbit anti-Narp under live conditions. As expected, GluR2 single transfected cells show no clusters larger than 50 pixels. In NP1/GluR2 expressing cells, only 2.3% $\pm$ 1.8% of GluR2 clusters are larger than 50 pixels. In contrast, in NP1/GluR2/Narp expressing cells, 16% $\pm$ 2.3% ($p < 0.001$) of GluR2 clusters are larger than 50 pixels. In each case, 20 transfected cells were randomly selected for analysis with Metamorph software.

transported to mossy fiber terminals where it coassembles with NP1.

Narp Enhances Clustering Activity of NP1

In assays of AMPAR coclustering in HEK 293 cells, Narp is substantially more effective than NP1. To test the hypothesis that addition of Narp can change the AMPAR clustering properties of NP1, we examined the effect of adding Narp to cells expressing NP1. Studies using COS cells (which we found to be technically superior to HEK 293 cells for cluster assays) are illustrated in Figure 6E. Consistent with results in HEK 293 cells, coexpression of GluR2 and NP1 produces small cell surface clusters that cocluster GluR2. When Narp was coexpressed with NP1 and GluR2, the size of NP1 clusters appears to increase and show enhanced coclustering of GluR2. To obtain a quantitative measure of this effect, we determined the percentage of GluR2 clusters that were larger than 50 pixels under each transfection condition. In cells expressing Narp, NP1-Myc, and HA-GluR2, 16% $\pm$ 3.5% of HA-GluR2 clusters are larger than 50 pixels. In contrast, in cells expressing NP1-Myc and HA-GluR2, only 2.3% $\pm$ 1.8% ($p < 0.001$) of clusters are larger than 50 pixels. In addition, in Narp/NP1-Myc/HA-GluR2 expressing cells, 19.6% $\pm$ 4.8% of NP1 clusters are larger than 50 pixels as compared to 2.5% $\pm$ 1.4% ($p < 0.001$) in NP1-Myc/HA-GluR2 expressing cells, indicating that NP1 cluster size is also enhanced by the addition of Narp to this complex. These studies indicate that addition of Narp increases the size of the pentraxin complex and increases its ability to cocluster AMPAR.

NP1 and Narp Show Distinct, Yet Supraadditive Synaptogenic Activities in Cultured Spinal Neurons

Expression of Narp transgene in cultured spinal neurons increases formation of excitatory synapses (O'Brien et al., 1999), while expression of a dominant-negative Narp suppresses synapse formation (O'Brien et al., 2002). Thus, spinal cord culture provides a validated model of synaptogenesis that is sensitive to increase or decrease of pentraxin. By selecting the neural elements that ex-

press the transgene, it is possible to assay the contribution of Narp when present in either axons or dendrites. Here, we use this assay to compare the synaptogenic activities of NP1 and Narp.

Cultured spinal neurons were transfected on day 3 in vitro with Narp-Myc or NP1-Myc, either separately or in combination, together with a control vector expressing the lacZ enzyme (controls). GFP-expressing vector was included to mark the axons and dendrites of transfected neurons. The correlation between transfection with GFP and Narp-Myc plasmid is routinely greater than 90%. Cultures were maintained for an additional 72–96 hr to assess the effect of transgene expression on ongoing synaptogenesis (O'Brien et al., 1997). Cultures were then fixed and stained with antibodies to the postsynaptic AMPA receptor subunit GluR2, as well as to the presynaptic vesicle protein synaptophysin. Additional coverslips were stained with antibodies to the postsynaptic glycine receptor scaffolding protein gephyrin, a marker for inhibitory synapses. An example of GluR2 staining of control and pentraxin transfected neurons is shown in Figure 7B.

After coding the slides, we identified axons of transfected spinal neurons and determined the likelihood of finding a cluster of the protein of interest (i.e., GluR2 or gephyrin) at junctions between transfected axons and dendrites from untransfected neurons. Untransfected cells were selected to be positive for GluR2 or gephyrin based on immunoreactivity at other positions along the dendrite. Results are reported in Figure 7A as probabilities; a score of 1.0 would indicate a cluster at each junction. As expected from previous reports (O'Brien et al., 1999), axons from neurons transfected with Narp show a significant increase in their ability to induce GluR2 clusters on contacted dendrites, compared to neurons transfected with a control vector (Figure 7A; 0.57 ± 0.03 versus 0.43 ± 0.06; $p < 0.05$). Likewise, axons from neurons transfected with NP1 show significantly increased AMPA receptor clustering, compared to control transfected neurons (0.51 ± 0.04; $p < 0.05$). Axons from neurons cotransfected with Narp and NP1 show increased association with GluR2 clusters compared to control or NP1 alone (0.61 ± 0.4; $p < 0.008$ for control and $p < 0.05$ for NP1). None of the constructs have any significant effect on the number of transfected axons associated with gephyrin clusters.

To compare Narp and NP1 effects on synaptogenesis when expressed postsynaptically, we determined the number of synaptic clusters of GluR2 on the dendrites of transfected neurons. As expected from previous results (O'Brien et al., 1999), neurons expressing Narp have more synaptic clusters of GluR2 than controls (Figure 7A, 8.4 ± 1.2 versus 6.3 ± 0.8; $p < 0.05$). The number of synaptic gephyrin clusters is unchanged. NP1 transgene expression has no detectable effect on the number of synapses associated with GluR2 (7.3 ± 0.5) or gephyrin. By contrast, dendrites of neurons that express both NP1 and Narp transgenes show a nearly 2-fold increase in GluR2 clusters compared to controls (10.9 ± 0.9, $p < 0.0001$). The effect of combined Narp and NP1 expression is greater than either alone ($p < 0.05$).

We conclude that NP1 possesses modest synaptogenic activity when expressed alone that is statistically significant in the present assay only when it is expressed in the presynaptic element. This does not exclude a role for NP1 as a postsynaptic factor but does illustrate a difference from Narp, which shows greater synaptogenic activity and is effective when expressed in either pre- or postsynaptic neurons. These results are consistent with observations from heterologous cells in which Narp forms larger clusters than NP1, and Narp clusters are more effective in coclustering GluR2 (Figure 5C). NP1 does enhance the postsynaptic synaptogenic activity of Narp. The supraadditive effect of Narp and NP1 is notable since simple mixing of these agents might have been predicted to produce an intermediate level of activity. The result is consistent with a model in which the pentraxin domains of Narp and NP1 are equally effective in interacting with AMPARs, and the N termini of these pentraxins mediate coassembly into complexes that possess properties distinct from NP1 alone.

Discussion

Mixed Pentraxin Assembly and Excitatory Synaptic Plasticity

The present study supports the hypothesis that NP1 and Narp contribute to a single pentraxin mechanism that plays a role in excitatory synaptic plasticity in developing and adult brain. We propose that the pentraxin agent is composed of NP1 and Narp, and the ratio of these proteins defines its synaptogenic activity (Figure 8). The N termini of Narp and NP1 interact and serve to generate a high-density array of oriented pentraxin domains that in turn interact with AMPAR or other proteins. Recent studies suggest that AMPAR may be relatively mobile when in the membrane at regions outside the synapse and become captured at the synapse (Borgdorff and Choquet, 2002). Narp and NP1 both selectively accumulate at excitatory synapses in primary hippocampal and spinal cord cultures and specifically coimmunoprecipitate AMPA receptors from brain. Both proteins are present selectively at excitatory synapses in mature brain where they are enriched in presynaptic elements and colocalize in vesicular-like structures. It is inferred from these localizations that their mechanisms of intracellular trafficking and secretion at excitatory synapses are similar, although in cultures, NP1 is relatively enriched at spine synapses. Narp and NP1 physically associate in a complex that is stable to SDS. Based on our understanding of the assembly of these proteins into a novel quaternary structure that is stabilized by position-specific disulfide linkages, we propose that the native complex in brain possesses a structure that is defined by these same physical properties.

Our model of pentraxin assembly rationalizes the effects of coexpressed Narp and NP1 in assays of excitatory synaptogenesis. NP1 is less effective at inducing excitatory synapses than Narp. NP1 forms smaller surface clusters and is also less effective than Narp at inducing clusters of AMPAR. This difference in clustering between Narp and NP1 is conferred by their N termini, which mediate assembly into disulfide-linked complexes. By contrast, the pentraxin domains of Narp and NP1 mediate interaction with AMPARs and appear comparable in this activity. Narp and NP1 coassemble into surface complexes that are larger than those of NP1

A. The Effect of Narp plus NP1 on Excitatory Synaptogenesis.

Experimental Design:

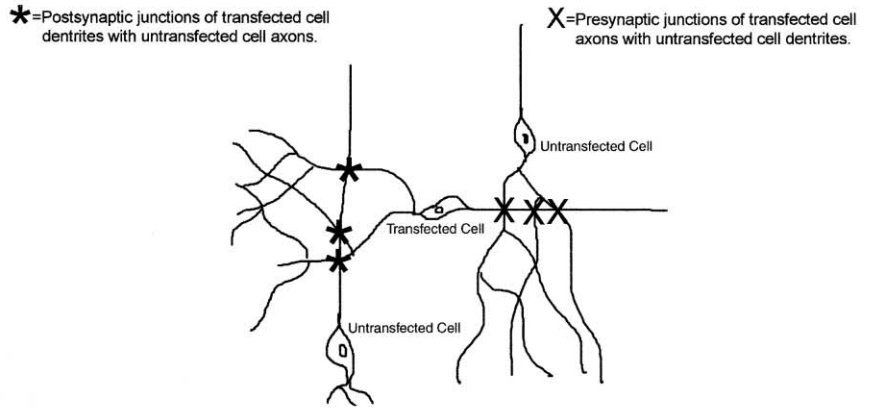

Transfected with	Control	NP-1	Narp	NP1 with Narp
Presynaptic (GluR2 Clusters/Contact; n=4)	0.43+/-0.06	0.51+/-0.04*	0.57+/-0.03*	0.61+/-0.04**
Presynaptic (Gephyrin Clusters/Contact; n=4)	0.33+/-0.07	0.35+/-0.06	0.38+/-0.08	0.31+/-0.06
Postsynaptic (Synaptic GluR2 Clusters/Cell; n=4)	6.30+/-0.80	7.30+/-0.50	8.40+/-1.20*	10.90+/-0.90***
Postsynaptic (Synaptic Gephyrin clusters/Cell;n=2)	7.90+/-0.80	6.80+/-0.70	7.30+/-1.40	7.10+/-0.70

* P<0.05 compared with control using paired t test.
** P<0.008 compared with control and P<0.05 compared with NP1 (but not Narp) alone using paired t test.
***P<$2X10^{-5}$ compared with control and P<0.05 compared with NP1 or Narp alone using paired t test.

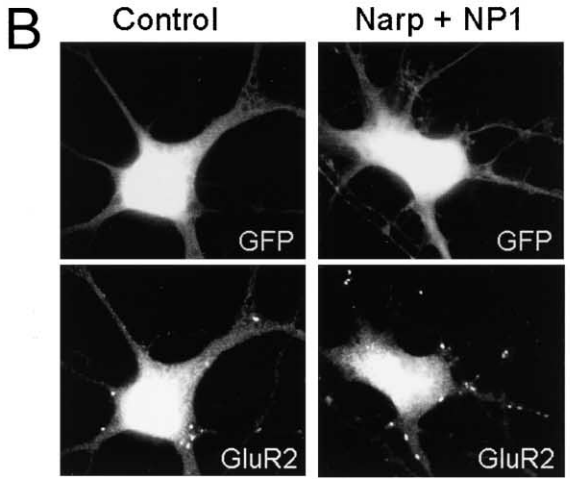

Figure 7. NP1 and Narp Cooperatively Enhance the Cluster Formation of Endogenous GluR2 on Spinal Neurons

(A) Quantification of the effect of pentraxins on synaptogenesis. The probability of postsynaptic GluR2 or gephyrin clusters associated with transfected presynaptic axons in each experimental condition was calculated (Presynaptic). In addition, the probability of dendritic clusters of GluR2 or gephyrin per site of axonal contact on a dendrite of a transfected neuron was also determined (Postsynaptic). The numbers shown are the mean of the four experiments, ±SD.

(B) E18 spinal neurons were transfected with Narp and NP1. These neurons were stained 2 days later to detect surface GluR2 distribution patterns. Transfected neurons showed enhanced GluR2 cluster formation as compared to untransfected controls.

alone and also more effective in coclustering AMPARs. By coassembling with NP1, Narp recruits NP1 into mixed pentraxin clusters that "present" an array of identically functional pentraxin domains that cluster AMPARs. In this model, Narp can recruit the nascent synaptogenic activity of NP1.

Pentraxins at the synapse appears to generate complexity based on mixing agents with distinct properties. Quantitative comparisons of Narp and NP1 expression in tissue indicate a range of at least 100-fold, with NP1 being the predominant pentraxin in developing brain and Narp becoming a stoichiometric partner in adult cortex and hippocampus later in development and during episodes of neuronal activity. These observations

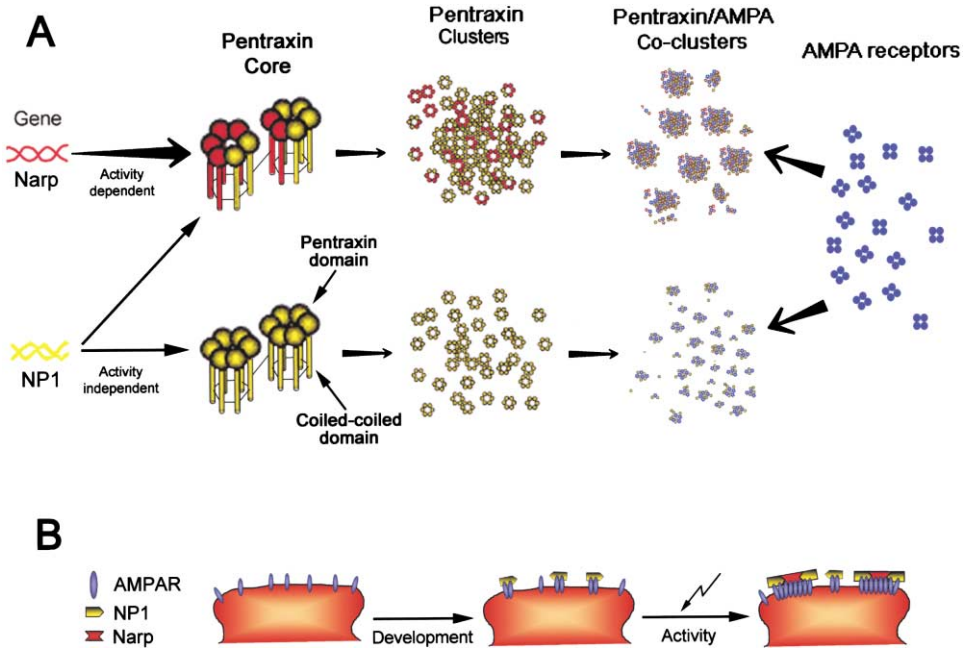

Figure 8. A Model for Pentraxin Function

(A) Narp and NP1 cofunction to induce AMPA receptor aggregation. NP1 is constitutively expressed in adult neurons and can form small cell surface clusters that can cocluster AMPA receptors. Activity-induced Narp expression results in the integration of Narp protein into NP1/Narp heteromultimers. These heteromultimers have an enhanced ability to cluster and to induce receptor coclustering.

(B) A hypothesis for pentraxin function at the synapse. Narp and NP1 function to aggregate AMPA receptors at synaptic sites. The differential regulation of the two pentraxins provides a mechanism by which the cell can tune the composition of the pentraxin agent and the degree of receptor clustering during development and in response to synaptic activity.

suggest that the composition of the pentraxin complex, and thus its synaptogenic activity, is tuned as a function of the activity history of the neuron.

A Novel Mechanism for Pentraxin Assembly

Determinants of SDS-stable Narp multimer formation were identified. Position-specific disulfide linkages are contributed by cysteines at positions 14, 26, and 79 of Narp. The specificity of interaction suggests that Narp molecules link in a parallel orientation. Narp cysteines 14 and 26 appear essential to the formation of the "core hexamer" species, while cysteine 79 appears to subserve a distinct role in assembly of higher mw species. By working with Narp mutants that can not form intermolecular disulfide linkages, we were also able to demonstrate a role in assembly for protein-protein interactions between predicted coiled-coil domains in the N terminus. These determinants of assembly stand in contrast to the assembly of classical pentraxins such as SAP and C-rp that assemble into pentamers and decamers based on interactions between pentraxin domains (Gewurz et al., 1995).

Studies of the combined assembly of Narp and NP1 provide additional insight into the quaternary structure of the pentraxin complex. Narp and NP1 associate by both protein-protein and disulfide mediated interactions. The predicted coiled-coil domains of Narp show 43% identity to NP1 and 29% identity to NPR (see below) but otherwise appear unique in surveys of public databases. Together with the present data, this suggests that the coiled-coil domains function to mediate specific multimerization between these neuronal pentraxins. As with Narp-Narp interactions, the Narp-NP1 interaction is robust and supports coimmunoprecipitation even in the absence of disulfide linkage.

NP1 and Narp also form disulfide-linked heteromultimers. The disulfide linkages between Narp and NP1 are mediated primarily by C14 of Narp, less so by C79, and not by C26. C26 of Narp shows remarkable specificity, interacting only with other Narp monomers and not NP1. Although our experiments examined pentraxins in solution, identical rules of assembly were confirmed for complexes present on the cell surface. Narp and NP1 form a SDS-stable association in brain. To our knowledge, the Narp/NP1 assembly is the first natural pentraxin complex that involves coassembly of different pentraxins. In proposing a molecular model we note that a mixed assembly of Narp and NP1 could lack stabilization afforded by C26 disulfide linkage. However, contiguous pairs of Narp linked by C26-C26 interaction could be integrated with NP1 without altering effective cross-linking. Specificity of the cysteine interactions may, therefore, affect the composition and position of pentraxins in mixed assemblies.

The protein termed neuronal pentraxin receptor (NPR) is another long-form pentraxin that is expressed in brain neurons and was cloned based on its association with NP1 and Narp in binding to taipoxin toxin (Dodds et al., 1997; Kirkpatrick et al., 2000). Like NP1 and Narp, NPR is predicted to possess an N-terminal coiled-coil domain and a C-terminal pentraxin domain. Like NP1, NPR shows alignment with cysteines at positions 14 and 79

of Narp; the position of the second cysteine, however, is not conserved among the three neuronal long-form pentraxins (Figure 4A). NPR is distinct from NP1 and Narp in that it possesses a single N-terminal membrane spanning domain and is predicted to form a membrane anchor for NP1 and Narp (Dodds et al., 1997). Alternative forms of NPR may also be secreted. Our present model would accommodate bimolecular or trimolecular complexes of NPR/NP1 and Narp.

Pentraxins Provide a Conserved Mechanism for Both Activity-Dependent and Activity-Independent Plasticity

How might pentraxins be involved in these synaptogenic events? Transgene expression of NP1 or Narp promotes clustering of synaptic AMPA receptors in culture and this process is known to be insensitive to tetrodotoxin or glutamate receptor blockage (O'Brien et al., 1997). In preliminary studies, we find that Narp secretion is not blocked by TTX but is blocked by tetanus toxin (D.X. and P.W., unpublished data). NP1 is prominently expressed in early postnatal forebrain and levels decline by a factor of ten between postnatal days 6 and 11. Coincident with the developmental decrease in NP1, there is a robust increase in Narp. While Narp is more active in culture assays of synaptogenesis, its developmental expression time course suggests NP1 is more relevant to early stages of synapse formation. Their reciprocal developmental expression coincides with the transition from early synaptogenesis, which is activity independent, to the later activity-dependent process. The observation that NP1 expression remains high in the adult brain suggests that activity-independent, secretion-dependent mechanisms may continue to contribute to synapse maintenance and remodeling. To our knowledge, this issue has not been examined. Mice with a targeted deletion of the NP1 gene have been reported to have no obvious CNS phenotype with the exception of a modest reduction in synaptophysin staining (Kirkpatrick et al., 2000). This may be attributable to functional redundancy of Narp.

In terms of current models, NP1 would be activity independent but secretion dependent and Narp would be activity dependent and secretion dependent. Vesicles with pentraxins, as detected by immunoEM, are not abundant at CNS synapses and do not appear to be conventional excitatory vesicles. Moreover, Narp and NP1 are not enriched in excitatory synaptic vesicle preparations (C. Hopf, S. Takamori, P.W., and R. Jahn, unpublished data). Thus, conventional assays of excitatory vesicle release may not correlate with pentraxin vesicle release. Future studies directed at the nature of the pentraxin vesicle and mechanism of secretion should be informative for understanding their contribution to synaptogenesis.

Experimental Procedures

Pentraxin Expression Constructs

The cloning of full-length Narp cDNA, its insertion into pRK5, and the addition of a Myc tag have been described previously (Tsui et al., 1996). Hexa-his tagged constructs were generated using PCR with Narp-pRK5 as a template and with the primers 5′-CCACTT TGCCTTTCTCTCC (from pRK5 sequence flanking cloned Narp cDNA) and 3′-GCTTCTCGCAGAGGACCTCAACGTGGTGGTGGTG GTGGTGATC**AGATCT**ATC. EcoRI (subcloning site used in the original cloned Narp cDNA) and XbaI sites (shown in bold face) contained in the PCR product were used to subclone into pRK5.

Full-length NP1 cDNA was cloned by screening a rat hippocampus oligo (dT)-primed cDNA library in UniZAP with a PCR-derived NP1 probe. The NP1 open reading frame, as published by Schlimgen et al. (1995), was amplified by PCR using primers 5′-GGTGCTCGAATT CTCCGCAGCC and 3′-GAAGCCTCTAGATCTGGCG and subcloned into pRK5 as described above. A C-terminal Myc-tag was added by PCR amplification using the same 5′-primer and XbaI containing primer 3′-TTTTTTCTAGAAATTGAGATCTTCCTCAGAAATGAGCTT TTGCTCCATGTTAACCTTGATCTGGCGGCAAGCCTCC.

The Narp cysteine mutants were generated using the QuiKChange Site-Directed Mutagenesis Kit (Stratagene). In each primer, the cysteine codon was replaced with a serine codon. Double and triple cysteine mutants [Narp (C14,26S)-Myc-PRK5; Narp (C14,79S)-Myc-pRK5; Narp (C26, 79S)-Myc-pRK5, and Narp (C14, 26, 79S)-Myc-pRK5] were generated using single (or double) cysteine mutants as the PCR template and amplifying with the primer containing the additional cysteine mutation.

Deletion constructs were made using the ExSite PCR-Based Site-Directed Mutagenesis Kit (Stratagene). Blunt ended PCR product which could then be religated and transformed into bacteria for subsequent selection of deletion clones. These clones were screened by restrictive digestion, DNA sequencing, and protein expression.

NP1/Narp chimeras were generated by amplifying the N-terminal half of Narp (aa 1–233) and the C-terminal half of NP1 (aa 236–432) separately by PCR, and the fragments were subcloned into pRK5 using an internal MluI site as well as EcoRI and XbaI restriction sites contained in the primers (5′-CGCTCGGGCATGCCCAGGATAACC and 3′-CCAGATGCATTCAAAGTGTCCCTCCCTC**TTCGAA**AAAAAAT CTAGAAAAAA for Narp-N; 5′-AAAAAAGAA**TTCGAA**CCAACTACAT GTATGCCAAGGTGAAG and 3′-GAAGCCTCTAGATCTGGCG for NP1-C). The two pentraxin pieces were subsequently joined by means of a silent BstBI introduced during PCR amplification (shown in bold face). Analogously, a NP1/Narp chimera encoding the N-terminal half of NP1 (aa 1–235) and the C-terminal half of Narp (aa 234–432) was generated using the following primers: 5′-GGTGCTCGAATTCTCCG CAGCC and 3′-GGAGACAAGTTTCAGCTGACATTCCCAC**TTCGAA** AAAAAATCTAGAAAAAA for NP1-N; 5′-AAAAAAGAA**TTCGAA**AC TACCTATACGGCAAGATCAAG and 3′-GGAGAAGGTATCTAGAAG TCCAGG for Narp-C.

The identity of all PCR-generated plasmid inserts was confirmed by DNA sequencing.

Cell Culture and Transfection

HEK 293 cell and primary neuronal culture transfection methods have been described previously (O'Brien et al., 1998, 1999). For protein assays in HEK 293 cells, 10 mls of 5×10^5 cells/ml were split 24 hr before transfection into a 100 mm culture tissue culture plate. For immunocytochemistry of COS cells, 2×10^5 cells were plated into each well of a 12-well tissue culture dish. For immunocytochemistry of neurons, E18 hippocampal neurons were grown at a low density of 2 to 4×10^4 cells/well on coverslips coated with poly-D lysine and laminin. Narp protein was expressed in HEK 293 cells by LipofectAMINE™ (Invitrogen) plasmid transfection. For immunocytochemistry and all experiments on primary cultured neurons, $CaPO_4$-based transfection methods were used (O'Brien et al., 1999).

Preparation, transfection, and quantitative evaluation of spinal cord cultures were performed as described previously (O'Brien et al., 1998, 1999, 2002).

Antibodies and Other Materials

The preparation of rabbit anti-Narp-specific antibody has been described previously (Tsui et al., 1996); goat anti-Narp antibody was prepared similarly. To prepare a rabbit and chicken anti-NP1, a NP1 fragment encoding amino acids 104 to 227 of the rat preprotein was PCR amplified using primers 5′-GAGGCCAGGATCCGGCGGCGGC and 3′-GAATGTCAGCGTCGACTTGTCTCC. It was linked to glutathione S-transferase (GST) in the pGEX-T2 (Pharmacia) vector using

BamHI and SalI sites contained in the primers. An antiserum specific for NP1 was prepared by immunization of rabbits with purified GST-NP1 fusion. For immunohistochemistry, NP1-specific antibodies were affinity purified on an immobilized fusion protein column. Preincubation of antibodies (at 100 μg/ml) with NP1 fusion protein (at 250 μg/ml) for 2 hr at 4°C efficiently blocked immunostaining.

Purified anti-GluR2, anti-GluR1, and anti-GluR6 antibodies were kind gifts from Dr. Richard Huganir. Mouse anti-*myc* McAb (9E10), mouse anti-HA 12CA5, anti-glutamic acid decarboxylase, mouse anti-synaptophysin McAb, rabbit anti-*myc*, rabbit anti-His were purchased from Roche. MAB 397 directed against GluR2 was from Chemicon. Fluorophore-labeled secondary antibodies for immunofluorescent staining were purchased from Jackson Immunoresearch. HRP-labeled secondary antibodies were purchased from Amersham Pharmacia Biotech.

Coimmunoprecipitations and Western Blotting

Coimmunoprecipitation assays addressing pentraxin and AMPARs interaction was performed as previously described (O'Brien et al., 1999). Coimmunoprecipitation assays addressing pentraxin disulfide bonding used the following wash protocols. Beads were washed twice with precooled immunoprecipitation buffer (1% Triton X-100, 10 mM sodium pyrophosphate, 1 mM sodium orthovanodate, and 0.1% PMSF in PBS [pH 7.4]), twice with PBS (pH 7.4), once with 0.5 M NaCl in PBS (pH 7.4), and twice with pH 7.4 PBS. Coimmunoprecipitation assays to distinguish from covalent and noncovalent pentraxin interactions required two additional washes with 0.5% SDS in PBS (pH 7.4). The washed beads were treated with loading buffer (125mM Tris [pH 6.8], 4% SDS, 20% glycerol, 0.016% bromophenol blue) at 65°C for 20 min.

Western Blot Analysis of Pentraxin Expression In Vivo

Examination of pentraxin expression during development and after MECS stimulation was performed on Sprague-Dawley rats. Samples were prepared as previously described (O'Brien et al., 1999).

Immunocytochemistry

Detailed procedures for live and permeablilized staining of heterologous cells and hippocampal neurons have been described (Mammen et al., 1997; O'Brien et al., 1999). For quantitative analysis of Narp-dependent AMPA receptor aggregation on the surface of transfected COS cells, digitized images were analyzed utilizing Metamorph software (Universal Imaging, Silver Springs, MD). To calculate the propensity of pentraxin molecules for forming cell surface aggregates (expressed as the fraction of Myc-positive cells that bear surface pentraxin clusters), COS cells were transfected with Myc-tagged pentraxin constructs. They were then stained alive with anti-pentraxin antisera, fixed, permeabilized, and counterstained with anti-*myc* antibody.

Immunohistochemistry of Brain

Three-month-old Sprague-Dawley rats were either treated with a single MECS or left untreated. Twenty-four hours after seizure administration, animals were anesthetized with pentobarbitol and perfused with 4% paraformaldehyde in PBS. Immunohistochemistry of brain was performed as previously described (O'Brien et al., 1999).

ImmunoEM was performed as previously described (Wang and Larsson, 1985; Petralia et al., 2001).

Affinity Chromatography of Narp for EM

Culture medium was harvested from 10 to 20 × 10 cm dish cultures of HEK 293 cells with transfected Myc-tagged Narp or Myc-tagged Narp mutants. This media was incubated with mouse anti-*myc* monoclonal antibody (9e10) covalently conjugated beads (200 μl) overnight at 4°C with rotation. The beads were washed according to the coimmunoprecipitation protocol described above. The remaining buffer was removed with two additional washes with 0.9% NaCl. The beads were loaded into a 1 ml column. The proteins were eluted in 0.15 M acetate buffer (pH 4.0) and were demonstrated to be essentially pure by comparison of silver stained SDS-PAGE and Western blot of the same material. The protein concentration of each sample was determined by measuring the UV light absorption at 260 nm and 280 nm. The concentration was calculated by formula: mg/ml = 1.45OD280 − 0.74OD260.

Electron Microscopy and Negative Staining

Discharged 400 mesh carbon coated Parlodion copper grid was floated on a 30 μl drop of purified Narp sample at 100 μg/ml to 150 μg/ml for 2 min. The sample grid was blotted with filter paper for drying. Two stainings were carried out in 1% Uranyl Acetate and 0.2% Tylose in distilled H_2O. The preparations were observed under a TEM (Hitachi CM 120) at 80 KV, and the images were photographed on Kodak 4489 EM film.

Acknowledgments

We would like to acknowledge Ya-Xian Wang for help in the preparations for the immunogold studies. Supported by National Institutes of Health grants R01-NSNS39156 (P.W.), KO2 MH01153 (P.W.), R01-NS37694 (R.J.O.), RO1-K02 53608 (R.J.O.), and grants ALTF-478 from EMBO (C.H.), the Christopher Reeve Paralysis Association, the Joseph and Esther Klingenstein Foundation, and the Center for ALS Research at Johns Hopkins.

Received: March 26, 2003
Revised: May 14, 2003
Accepted: June 24, 2003
Published: July 30, 2003

References

Biederer, T., Sara, Y., Mozhayeva, M., Atasoy, D., Liu, X., Kavalali, E.T., and Sudhof, T.C. (2002). SynCAM, a synaptic adhesion molecule that drives synapse assembly. Science *297*, 1525–1531.

Borgdorff, A.J., and Choquet, D. (2002). Regulation of AMPA receptor lateral movements. Nature *417*, 649–653.

Bose, C.M., Qiu, D., Bergamaschi, A., Gravante, B., Bossi, M., Villa, A., Rupp, F., and Malgaroli, A. (2000). Agrin controls synaptic differentiation in hippocampal neurons. J. Neurosci. *20*, 9086–9095.

Bruses, J.L. (2000). Cadherin-mediated adhesion at the interneuronal synapse. Curr. Opin. Cell Biol. *12*, 593–597.

Cantallops, I., Haas, K., and Cline, H.T. (2000). Postsynaptic CPG15 promotes synaptic maturation and presynaptic axon arbor elaboration in vivo. Nat. Neurosci. *3*, 1004–1011.

Craig, A.M., Blackstone, C.D., Huganir, R.L., and Banker, G. (1994). Selective clustering of glutamate and gamma-aminobutyric acid receptors opposite terminals releasing the corresponding neurotransmitters. Proc. Natl. Acad. Sci. USA *91*, 12373–12377.

Dalva, M.B., Takasu, M.A., Lin, M.Z., Shamah, S.M., Hu, L., Gale, N.W., and Greenberg, M.E. (2000). EphB receptors interact with NMDA receptors and regulate excitatory synapse formation. Cell *103*, 945–956.

Dodds, D.C., Omeis, I.A., Cushman, S.J., Helms, J.A., and Perin, M.S. (1997). Neuronal pentraxin receptor, a novel putative integral membrane pentraxin that interacts with neuronal pentraxin 1 and 2 and taipoxin-associated calcium-binding protein 49. J. Biol. Chem. *272*, 21488–21494.

Emsley, J., White, H.E., O'Hara, B.P., Oliva, G., Srinivasan, N., Tickle, I.J., Blundell, T.L., Pepys, M.B., and Wood, S.P. (1994). Structure of pentameric human serum amyloid component. Nature *367*, 338–345.

Ethell, I.M., and Yamaguchi, Y. (1999). Cell surface heparan sulfate proteoglycan syndecan-2 induces the maturation of dendritic spines in rat hippocampal neurons. J. Cell Biol. *144*, 575–586.

Ethell, I.M., Irie, F., Kalo, M.S., Couchman, J.R., Pasquale, E.B., and Yamaguchi, Y. (2001). Ephb/syndecan-2 signaling in dendritic spine morphogenesis. Neuron *31*, 1001–1013.

Ferreira, A. (1999). Abnormal synapse formation in agrin-depleted hippocampal neurons. J. Cell Sci. *112*, 4729–4738.

Gewurz, H., Zhang, X.H., and Lint, T.F. (1995). Structure and function of the pentraxins. Curr. Opin. Immunol. *7*, 54–64.

Hsu, Y.C., and Perin, M.S. (1995). Human neuronal pentraxin II

(NPTX2): conservation, genomic structure, and chromosomal localization. Genomics *28*, 220–227.

Kandel, E.R. (2001). The molecular biology of memory storage: a dialogue between genes and synapses. Science *294*, 1030–1038.

Kirkpatrick, L.L., Matzuk, M.M., Dodds, D.C., and Perin, M.S. (2000). Biochemical interactions of the neuronal pentraxins. Neuronal pentraxin (NP) receptor binds to taipoxin and taipoxin-associated calcium-binding protein 49 via NP1 and NP2. J. Biol. Chem. *275*, 17786–17792.

Lupas, A., Van Dyke, M., and Stock, J. (1991). Predicting coiled coil from protein sequences. Science *252*, 1162–1164.

Mammen, A.L., Huganir, R.L., and O'Brien, R.J. (1997). Redistribution and stabilization of cell surface glutamate receptors during synapse formation. J. Neurosci. *17*, 7351–7358.

McMahan, U.J. (1990). The agrin hypothesis. Cold Spring Harb. Symp. Quant. Biol. *55*, 407–418.

Missler, M., and Sudhof, T.C. (1998). Neurexins: three genes and 1001 products. Trends Genet. *14*, 20–26.

Nedivi, E., Wu, G.Y., and Cline, H.T. (1998). Promotion of dendritic growth by CPG15, an activity-induced signaling molecule. Science *281*, 1863–1866.

O'Brien, R.J., Mammen, A.L., Blackshaw, S., Ehlers, M.D., Rothstein, J.D., and Huganir, R.L. (1997). The development of excitatory synapses in cultured spinal neurons. J. Neurosci. *17*, 7339–7350.

O'Brien, R.J., Lau, L.F., and Huganir, R.L. (1998). Molecular mechanisms of glutamate receptor clustering at excitatory synapses. Curr. Opin. Neurobiol. *8*, 364–369.

O'Brien, R.J., Xu, D., Petralia, R.S., Steward, O., Huganir, R.L., and Worley, P. (1999). Synaptic clustering of AMPA receptors by the extracellular immediate-early gene product Narp. Neuron *23*, 309–323.

O'Brien, R., Xu, D., Mi, R., Tang, X., Hopf, C., and Worley, P. (2002). Synaptically targeted narp plays an essential role in the aggregation of AMPA receptors at excitatory synapses in cultured spinal neurons. J. Neurosci. *22*, 4487–4498.

Petralia, R.S., Wang, Y.X., Sans, N., Worley, P.F., Hammer, J.A., III, Wenthold, R.J. (2001). Glutamate receptor targeting in the postsynaptic spine involves mechanisms that are independent of myosin Va. Eur. J. Neurosci. *13*, 1722–1732.

Rao, A., Harms, K.J., and Craig, A.M. (2000). Neuroligation: building synapses around the neurexin-neuroligin link. Nat. Neurosci. *3*, 747–749.

Sanes, J.R., and Lichtman, J.W. (2001). Induction, assembly, maturation and maintenance of a postsynaptic apparatus. Nat. Rev. Neurosci. *2*, 791–805.

Scheiffele, P., Fan, J., Choih, J., Fetter, R., and Serafini, T. (2000). Neuroligin expressed in nonneuronal cells triggers presynaptic development in contacting axons. Cell *101*, 657–669.

Schlimgen, A.K., Helms, J.A., Vogel, H., and Perin, M.S. (1995). Neuronal pentraxin, a secreted protein with homology to acute phase proteins of the immune system. Neuron *14*, 519–526.

Serpinskaya, A.S., Feng, G., Sanes, J.R., and Craig, A.M. (1999). Synapse formation by hippocampal neurons from agrin-deficient mice. Dev. Biol. *205*, 65–78.

Shrive, A.K., Cheetham, G.M., Holden, D., Myles, D.A., Turnell, W.G., Volanakis, J.E., Pepys, M.B., Bloomer, A.C., and Greenhough, T.J. (1996). Three-dimensional structure of human C-reactive protein. Nat. Struct. Biol. *3*, 346–354.

Tsui, C.C., Copeland, N.G., Gilbert, D.J., Jenkins, N.A., Barnes, C., and Worley, P.F. (1996). Narp, a novel member of the pentraxin family, promotes neurite outgrowth and is dynamically regulated by neuronal activity. J. Neurosci. *16*, 2463–2478.

Wang, B.L., and Larsson, L.I. (1985). Simultaneous demonstration of multiple antigens by indirect immunofluorescence or immunogold staining. Novel light and electron microscopic double and triple staining method employing primary antibodies from the same species. Histochemistry *83*, 47–56.

Yagi, T., and Takeichi, M. (2000). Cadherin superfamily genes: functions, genomic organization, and neurologic diversity. Genes Dev. *14*, 1169–1180.

Zhu, J.J., Esteban, J.A., Hayashi, Y., and Malinow, R. (2000). Postnatal synaptic potentiation: delivery of GluR4-containing AMPA receptors by spontaneous activity. Nat. Neurosci. *3*, 1098–1106.

Ziv, N.E., and Garner, C.C. (2001). Principles of glutamatergic synapse formation: seeing the forest for the trees. Curr. Opin. Neurobiol. *11*, 536–543.